Ch 09
Rheology of entangled polymers

Entanglements

no excluded volume effect -> configuration distribution is Gaussian
no hydrodynamic interaction

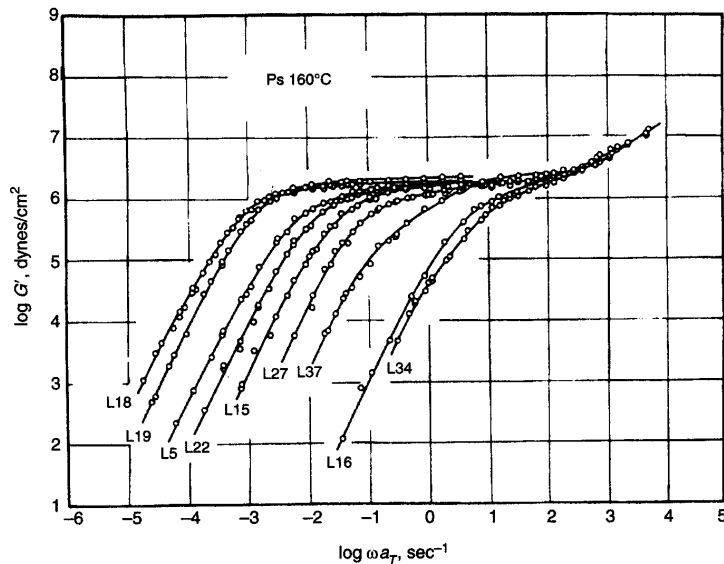$$M_c < M_e = \frac{\rho N_A}{\nu} = \frac{4}{5} \frac{\rho N_A k_B T}{G_N^0}$$

Figure 3.22 Storage modulus, G', as a function of frequency reduced to 160°C for nearly monodisperse polystyrenes of molecular weight ranging from 580,000 to 47,000, from left to right. (Reprinted with permission from Onogi et al., Macromolecules 3:109. Copyright 1970, American Chemical Society.)
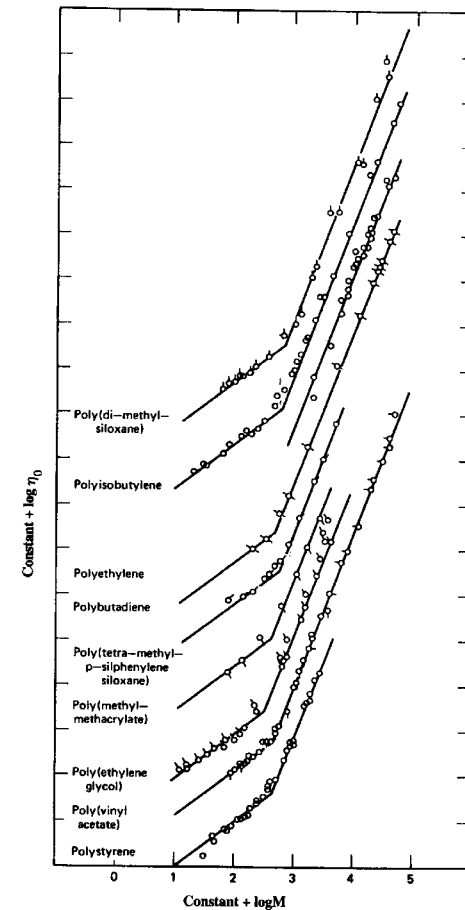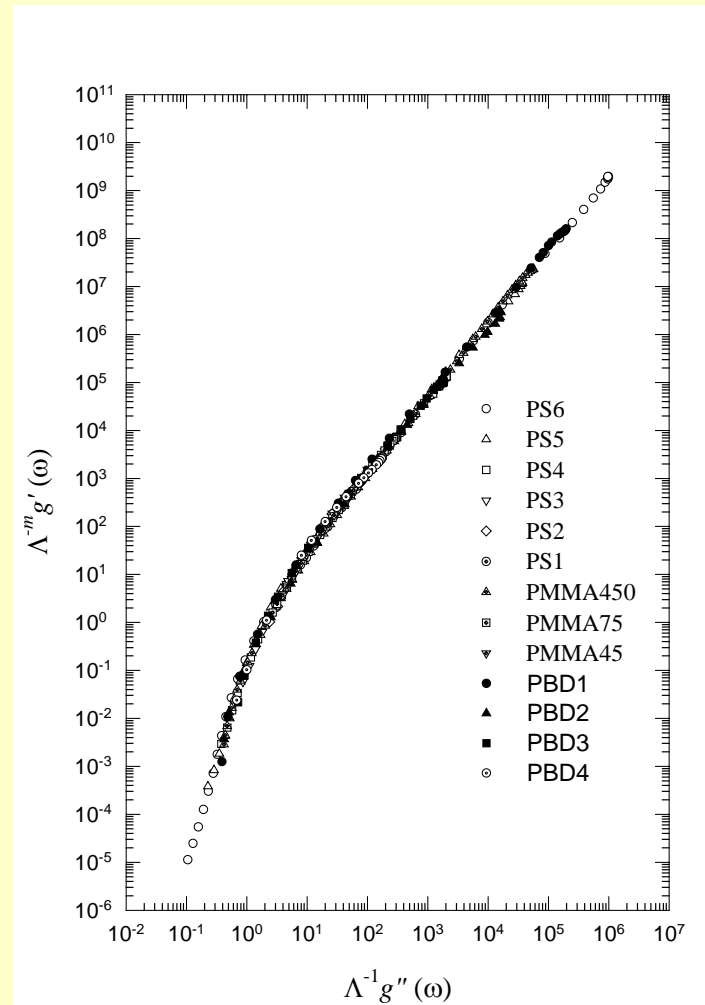

Figure 3.3 Relationship between zero-shear viscosity and molecular weight for several nearly monodisperse melts. For clarity, the curves are shifted relative to each other along both the abscissa and ordinate. (From Berry and Fox 1968, reprinted with permission from Springer Verlag.)

Universal behavior

$$g' \equiv \frac{G'}{J_e^0 \eta_0^2 \omega^2}, \quad g'' \equiv \frac{G''}{\eta_0 \omega}$$
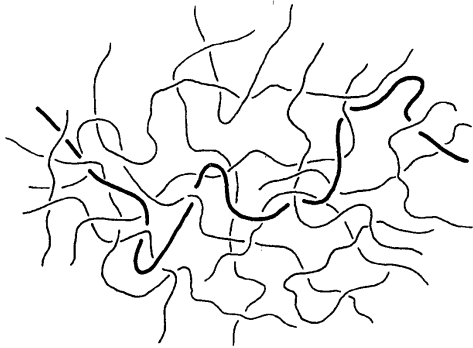
Reptation

$$\eta_o \sim M^3$$

Figure 3.23 A polymer molecule entangled in a mesh of other polymer chains. (From Graessley 1982, reprinted with permission from Springer Verlag.)

(A)   **(B)**   **(C)**

Figure 3.24   **(A)** A polymer molecule is entangled with neighboring molecules that **(B)** confine the given chain to a tube-like region. **(C)** The tube contour is roughly that of a random walk with step size equal to the tube diameter, a. This random walk is called the *primitive path*; its contour length is much less than the contour length of the chain itself. (From Graessley 1982, reprinted with permission from Springer Verlag.)
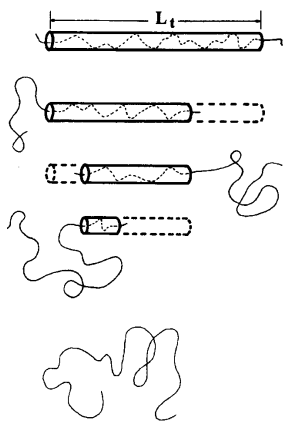

Figure 3.25   Reptation of a polymer molecule out of its tube, where, to aid visualization, the tube of Fig. 3-24 has been "straightened out." (From Graessley 1982, reprinted with permission from Springer Verlag.)
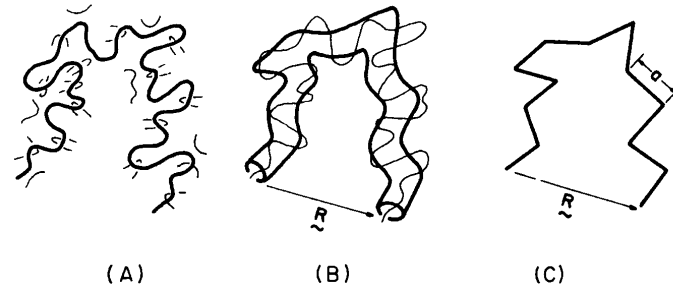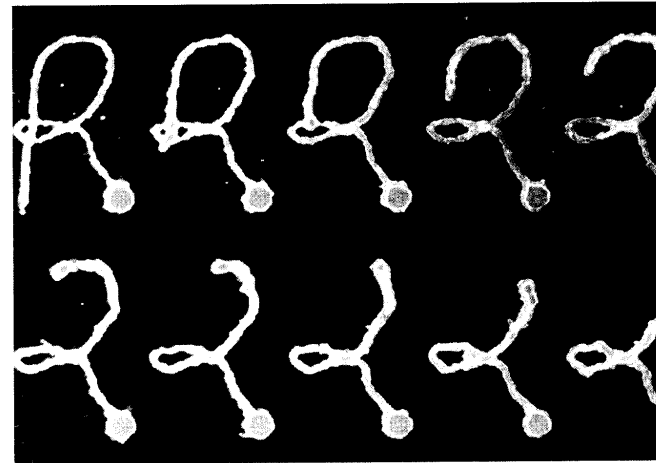

Figure 3.4   Time sequence of images showing retraction of one end of a fluorescing 60-μm-long DNA molecule entangled in a solution of other, non-fluorescing DNA molecules. The fluorescing molecule was attached at one end to a small sphere that was pulled through the solution using a laser-optical trap, to form the letter R. The free end then retracts through a "tube-like" region formed by the surrounding mesh of other, invisible DNA chains. (Reprinted with permission from the cover of *Science*, May 6, 1994; Copyright 1994, American Association for the Advancement of Science.)

Non-reptative relaxation mechanisms
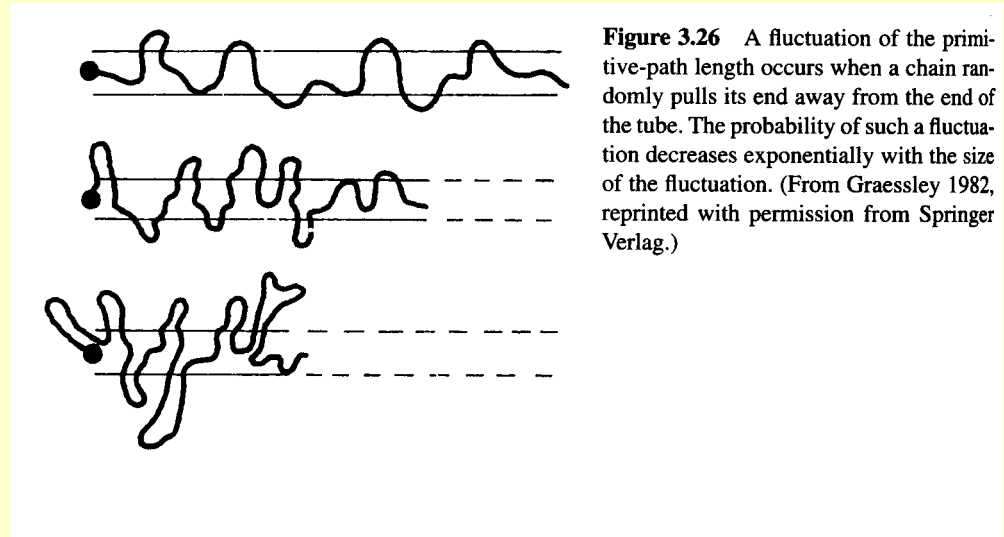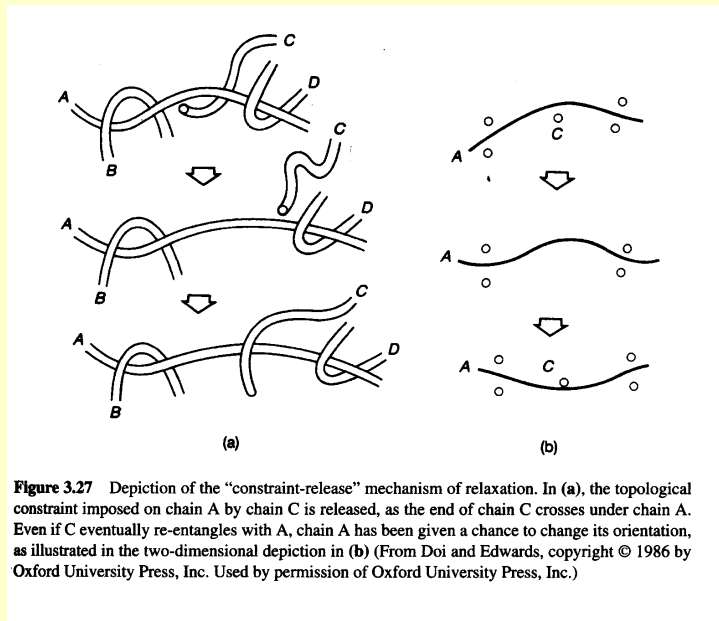
Primitive path fluctuations ->

Figure 3.26 A fluctuation of the primitive-path length occurs when a chain randomly pulls its end away from the end of the tube. The probability of such a fluctuation decreases exponentially with the size of the fluctuation. (From Graessley 1982, reprinted with permission from Springer Verlag.)

<- Constraint release

(a)   (b)

Figure 3.27 Depiction of the "constraint-release" mechanism of relaxation. In (a), the topological constraint imposed on chain A by chain C is released, as the end of chain C crosses under chain A. Even if C eventually re-entangles with A, chain A has been given a chance to change its orientation, as illustrated in the two-dimensional depiction in (b) (From Doi and Edwards, copyright © 1986 by Oxford University Press, Inc. Used by permission of Oxford University Press, Inc.)

Doi-Edwards theory

Linear relaxation modulus

a fraction of the original tube remains unvacated after time t

$$P(t) = \sum_{i \text{ odd}} \frac{8}{\pi^2 i^2} \exp\left[\frac{-i^2 t}{\tau_d}\right]$$

linear relaxation modulus

$$G(t) = \sum_{i \text{ odd}} G_i \exp\left[-t/\tau_i\right], \quad G_i = 8G_N^0/\pi^2 i^2, \quad \tau_i = \tau_d/i^2$$

storage and loss moduli

$$G'(\omega) = \sum_i G_i \frac{\omega^2 \tau_i^2}{1 + \omega^2 \tau_i^2} \qquad G''(\omega) = \sum_i G_i \frac{\omega \tau_i}{1 + \omega^2 \tau_i^2}$$
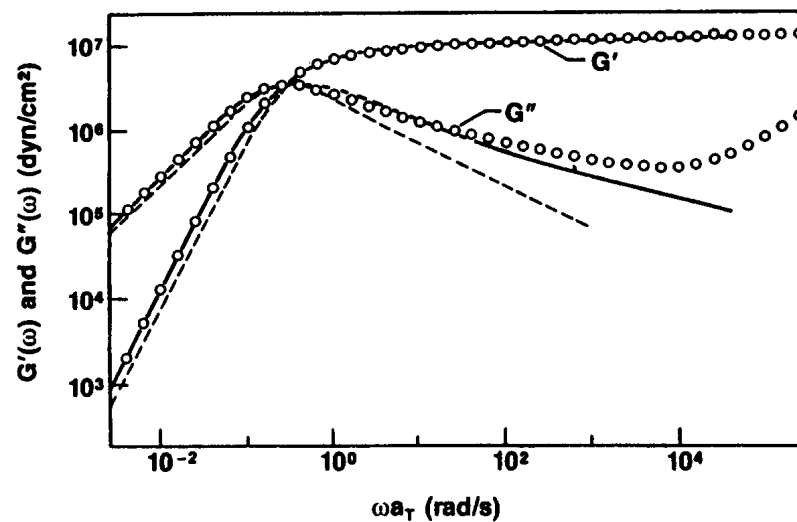

Figure 3.29 Linear moduli G' and G'' versus frequency shifted via time–temperature superposition to 27°C for a polybutadiene melt of molecular weight 360,000 and of low polydispersity. The dashed line is the prediction of reptation theory given by Eq. (3-67); the solid line includes effects of fluctuations in the length of the primitive path. (From Pearson 1987.)

Doi-Edwards theory

Nonlinear modulus and damping function

time-strain separability $\qquad G(t,\gamma) = G(t)h(\gamma)$
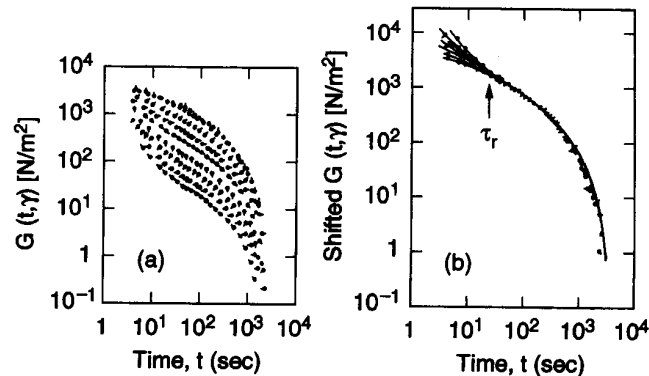
incomplete retraction

Figure 3.30 (a) The nonlinear shear relaxation modulus $G(t,\gamma)/\gamma$ as a function of time for various strain amplitudes for a 20% concentrated solution of polystyrene of molecular weight 1.8×10^6 in chlorinated diphenyl. Each curve corresponds to a different strain, ranging from 0.41 to 25.4, with the lower curves corresponding to the higher strains. (b) The curves are superimposed at times longer than $\tau_r = 20$ sec via vertical shifting by an amount $h(\gamma)$ plotted in Fig. 3-31. (From Einaga et al. 1971, with permission from the Society of Polymer Science, Japan.)

Independent alignment approximation: after retraction, each strand is oriented independently of the others, and the change in orientation produced by retraction is neglected.

Doi-Edwards theory

Constitutive equation

$$\boldsymbol{\sigma} = \int_{-\infty}^{t} m(t-t')\mathbf{Q}(t',t)dt' \qquad \mathbf{Q} \equiv 5\left\langle \frac{\mathbf{u}'\cdot\mathbf{E}\mathbf{u}'\cdot\mathbf{E}}{\left|\mathbf{u}'\cdot\mathbf{E}\right|^2} \right\rangle_0$$

$$m(t-t') \equiv \frac{d}{dt'}G(t-t') \qquad G(t) = \sum_{i\ odd} G_i \exp\left[-t/\tau_i\right], \quad G_i = 8G_N^0/\pi^2 i^2, \quad \tau_i = \tau_d/i^2$$

Separable K-BKZ equation

$$\boldsymbol{\sigma} = \int_{-\infty}^{t} m(t-t')\left[\phi_1(I_1,I_2)\mathbf{B}(t',t)+\phi_2(I_1,I_2)\mathbf{C}(t',t)\right]dt' \qquad \phi_1 = 2\frac{\partial U}{\partial I_1}, \quad \phi_2 = -2\frac{\partial U}{\partial I_2},$$

Curie approximation

$$U(I_1,I_2) \approx \frac{5}{2}\ln\left(\frac{J-1}{7}\right) \qquad J \equiv I_1 + 2\left(I_2 + 13/4\right)^{1/2}$$

$$\mathbf{Q} \approx \left(\frac{5}{J-1}\right)\mathbf{B} - \left(\frac{5}{(J-1)(I_2+13/4)^{1/2}}\right)\mathbf{C}$$

Differential approximation

$$\overset{\nabla}{\boldsymbol{\sigma}} + \frac{2}{3G}\mathbf{D}:\boldsymbol{\sigma\sigma} + \frac{1}{\tau}\left(\boldsymbol{\sigma}-G\boldsymbol{\delta}\right) = \mathbf{0}$$
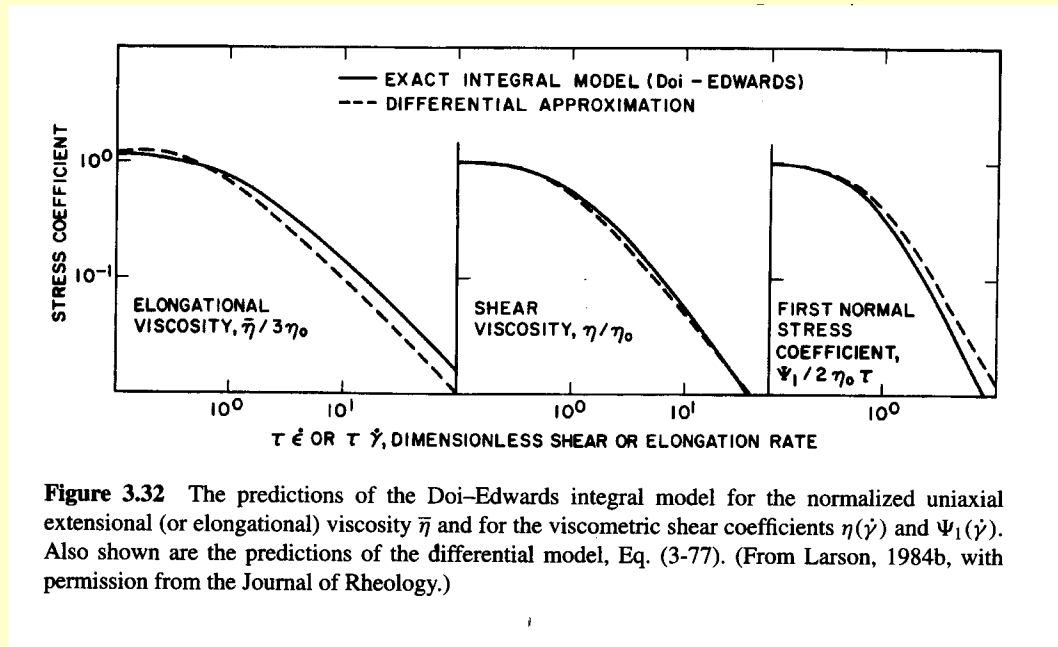
Prediction of reptation theory

Figure 3.32 The predictions of the Doi–Edwards integral model for the normalized uniaxial extensional (or elongational) viscosity $\bar{\eta}$ and for the viscometric shear coefficients $\eta(\dot{\gamma})$ and $\Psi_1(\dot{\gamma})$. Also shown are the predictions of the differential model, Eq. (3-77). (From Larson, 1984b, with permission from the Journal of Rheology.)

$$\eta \sim \dot{\gamma}^{-1.5}, \quad \Psi_1 \sim \dot{\gamma}^{-2} \quad \text{Predicts extreme thinning}$$

$$\eta \sim \dot{\gamma}^{-0.82}, \quad \Psi_1 \sim \dot{\gamma}^{-1.5} \quad \text{Experiments}$$
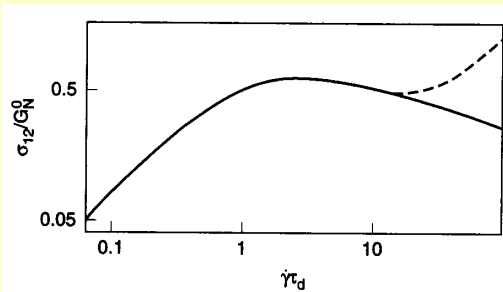
Prediction of reptation theory

Figure 3.33 The solid curve is the dimensionless shear stress σ_{12}/G_N^0 versus dimensionless shear rate $\dot{\gamma}\tau_d$ predicted by the Doi–Edwards constitutive equation, Eq. (3-71). The dashed curve adds a speculated contribution to the stress from Rouse modes. (From Doi and Edwards 1979, reproduced by permission of The Royal Society of Chemistry.)
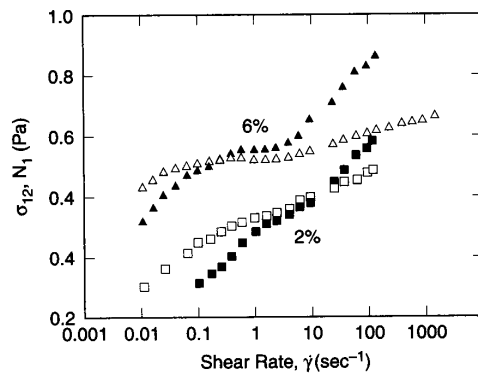

Figure 3.34 Shear stress (open symbols) and first normal stress difference (closed symbols) as functions of shear rate for two solutions of very-high-molecular-weight polymethylmethacrylate ($M = 23.8 \times 10^6$) in toluene at a concer g/dL (squares) and 6 gm/ (From Bercea et al. 1993 sion.)

Stress maximun leads to material instability

Fast flow convects away the polymer molecules containing a given chain, and destroys the tube surrounding that chain, faster than the chain itself can reptate out of the tube.
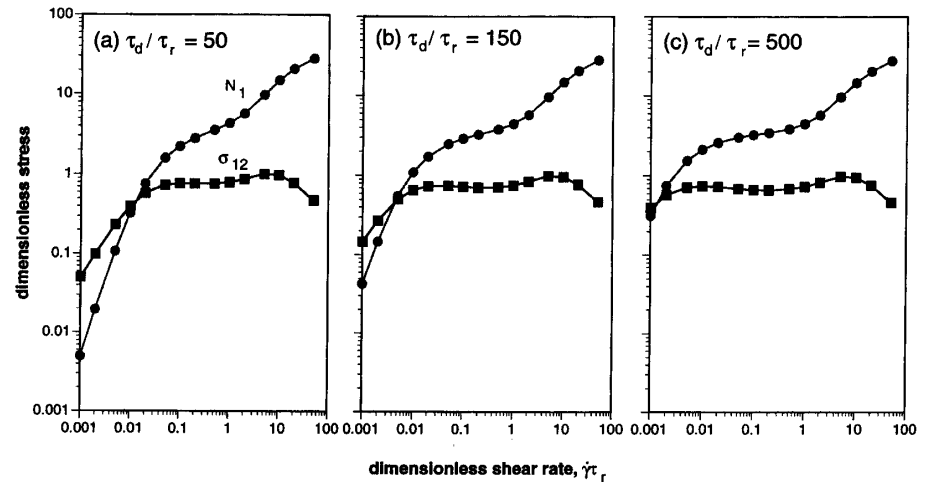
Convective constraint release ->

Figure 3.35 Steady-state values of the reduced shear stress σ_{12}/G_N^0 and first normal stress difference N_1/G_N^0 as functions of dimensionless shear rate $\dot{\gamma}\tau_r$ predicted by the equations of a constraint-release reptation theory (see Problem 3.10) for $\tau_d/\tau_r =$ (a) 50, (b) 150, and (c) 500, where τ_d is the reptation time and τ_r is the Rouse retraction time. See also Marracci and Ianniruberto (1997). (From Larson et al. 1998, with permission.)

Semiempirical constitutive equations

Integral type
$$\boldsymbol{\sigma} = \int_{-\infty}^{t} m(t-t')\left[\phi_1(I_1,I_2)\mathbf{B}(t',t) + \phi_2(I_1,I_2)\mathbf{C}(t',t)\right]dt'$$

$$\phi_1 = f_1 e^{-n_1\sqrt{I-3}} + f_2 e^{-n_2\sqrt{I-3}}, \quad \phi_2 = 0, \quad with \quad I = \alpha I_1 + (1-\alpha)I_2 \qquad \text{Wagner model}$$

$$\phi_1 = \frac{1}{\alpha(I_1-3) + b(I_2-3)}, \quad \phi_2 = 0 \qquad \text{Papanastasiou model}$$

Differential type
$$\overset{\triangledown}{\boldsymbol{\sigma}} + \frac{1}{\tau}\boldsymbol{\sigma} + \mathbf{G}(\boldsymbol{\sigma},\mathbf{D}) + H(\boldsymbol{\sigma}) = 2G\mathbf{D}$$

$$\mathbf{G} = \xi(\mathbf{D}\cdot\boldsymbol{\sigma} + \boldsymbol{\sigma}\cdot\mathbf{D}), \quad \mathbf{H} = \mathbf{0} \quad (\textit{Johnson and Segalman } 1977)$$

$$\mathbf{G} = \mathbf{0}, \quad \mathbf{H} = \alpha\frac{1}{\tau G}\boldsymbol{\sigma}:\boldsymbol{\sigma} \quad (\textit{Giesekus } 1966, 1982)$$

$$\mathbf{H} = \frac{1}{\tau}\left[\exp\left(\frac{\alpha}{G}tr\boldsymbol{\sigma}\right) - 1\right]\boldsymbol{\sigma} \quad (\textit{Phan-Thien and Tanner } 1977, 1978)$$

$$\mathbf{G} = \frac{2}{3}\frac{\alpha}{G}\mathbf{D}:\boldsymbol{\sigma}(\boldsymbol{\sigma} + G\boldsymbol{\delta}), \quad \mathbf{H} = \mathbf{0} \ (\textit{Larson } 1984b)$$

$$\mathbf{G} = \alpha(2\mathbf{D}:\mathbf{D})^{1/2}\boldsymbol{\sigma}, \quad \mathbf{H} = \mathbf{0} \ (\textit{White and Metzner } 1963)$$